Performance Studies of a Colloid Thruster System[*‡]

Freddy M. Pranajaya and Mark A. Cappelli
Thermosciences Division, Mechanical Engineering Department
Stanford University
Building 520
Stanford, CA 94309-3032
650-725-2069 / 650-725-2020
freddyp@stanford.edu / cap@stanford.edu

IEPC 01-284

Preliminary results are presented, of measurements of thrust (T) and specific impulse (I_{sp}), produced by a single emitter prototype colloid propulsion system. The development of the colloid thruster propulsion package at Stanford University is in preparation for flight-testing on a 20-kg university nanosatellite, to be launched in 2003. The half-kilogram Colloid Micro Thruster (CMT) package measures 10 cm x 10 cm x 20 cm, consumes 6 watts of maximum power for all on-board functions (including power processing, and microprocessor control system), and stores and provides controlled delivery of 10 ml of 2.0 M sodium-iodide/glycerol propellant to the emission source. The prototype unit tested here is highly modular, to allow testing of multiple thruster "core" designs. Here we report on the performance of a single-emitter core, consisting of a 150 μm OD / 75 μm ID stainless-steel capillary needle charged to as high as 6 kV relative to the extractor which is maintained at spacecraft ground potential. The measured emission current is found to be exponentially dependent on the applied acceleration voltage, placing it outside of regimes studied previously. Performance mapping, carried out by two indirect methods of determining T and I_{sp} (from steady-state measurements of current and mass flow, and from time-of flight measurements) indicates operation at a level of I_{sp} = 200 sec and T = 4 μN – somewhat below design targets, due largely to the relatively low applied voltage used (~4.5 kV). A discussion is presented about interesting dynamical behavior seen at emission onset, when current "bursts" are observed.

Introduction

Space mission designers have long been relying on electric propulsion because of its high specific impulse, allowing higher total ΔV, which makes it suitable for long space missions or for spacecraft with limited fuel storage capacity. Despite this advantage, the high power consumption and specialized power supply requirements have made electric propulsion options unattractive for Class I (5-20 kg) and Class II (1-5 kg) spacecraft.

Colloid micro-thruster (CMT) technology is expected to satisfy the need for high-performance propulsion units for small spacecraft. In a recent review paper, [1] it was suggested that of all the micro-electric primary propulsion options reviewed, colloid thrusters were believed to be the most suited for microsatellite propulsion applications. Previous research has already demonstrated that colloid propulsion technology has significant potential [1], although it has not nearly reached the level of maturity in its development as have other electric rocket technologies. It is also apparent from a review of the colloid rocket literature [2-7], that there is much work to be done on developing an understanding of the fundamental processes involved in the formation and acceleration

[*] Presented as Paper IEPC-01-284 at the 27th International Electric Propulsion Conference, Pasadena, CA, 15-19 October 2001.

of the electrospray, and in the characterizing of the emission process. Furthermore, there is little or no research on the on miniaturizing this technology so that it may be made suitable for micro- and nanosatellite propulsion applications, and, equally important, on the integration of this technology for flight. Current as well as future research efforts are motivated primarily by the need from the micro- and nanosatellite community, and by the need for a high-performance, economical propulsion option for advanced missions utilizing a formation (cluster) of multiple spacecraft.

In this paper, we present our continuing efforts in the development and characterization of colloid micropropulsion concepts, with a focus on the behavior of a prototype flight system that is to fly on an upcoming nanosatellite mission (EMERALD nanosatellite project - a joint project between Stanford University and Santa Clara University, funded through the Air Force Research Laboratory University Nanosatellite Program). This paper focuses largely on our recent efforts to measure, albeit indirectly, the thrust and specific impulse of a single-needle emission source. Both steady-state measurements of extracted beam current and mass flow rate, as well as time-of-flight methods are used to measure the thrust and specific impulse. The thrust levels achieved with a single emitter source are within those expected based on the scaling of studies of higher power sources in the early U.S. literature [2,5]. However, an extension to multiple emitter sources has proved to be problematic due to the conventional manufacturing and assembly processes used to construct our flight prototype.

Background

Theory

The application of a high voltage relative to a metal capillary tube containing a weakly conducting liquid causes the meniscus of the liquid to form so-called "Taylor cones" [7-9], the apex of which discharges a charge-carrying micro-jet of high velocity (see **Figure 1**). At sufficiently high voltages, the micro-jet becomes unstable very near the apex, and breaks up into charged droplets (hence the name "colloid"), the size and charge of which are determined approximately by a balance between surface tension, and surface charge repulsion. These charged droplets accelerating due to the applied potential (or electric field) may break-up further into secondary droplets. When used as an ion rocket, the high velocity charged droplets generated by the source impart a recoil momentum to the spacecraft as they are "exhausted" or leave the region of high electric field (separate from the field lines) by passing through an extractor orifice.

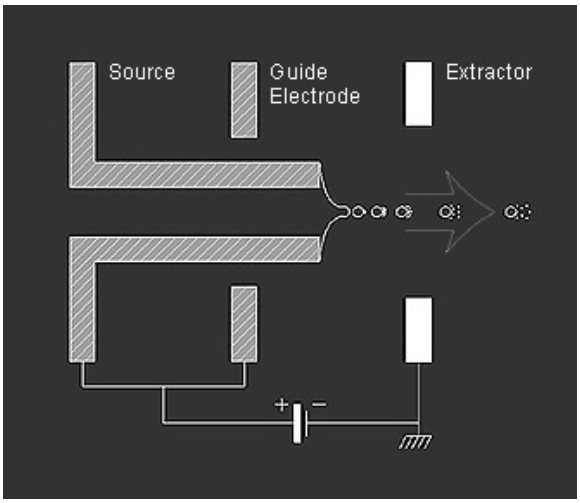

Figure 1. Schematic of Single-Emitter Core.

The shaping of the applied electric field can control the trajectories of the charged droplets. As shown in **Figure 1**, the divergence of the field lines can be minimized by the addition of so-called guide electrodes, held at the same potential as the emitter, although it is difficult to avoid any radial component in the electric field due to the presence of the extractor orifice. In practice, the applied voltage on the needle capillary is positive relative to ground, so as to emit positively charged jets. The steady emission of a positive jet, and eventually, positively-charged droplets require the subsequent emission of electrons from the rocket, to preserve charge on the spacecraft. The electron neutralizer (not shown in the figure) can be a simple resistively heated filament located just downstream of the extractor orifice.

The governing equations for the thrust, T, and specific impulse, I_{sp}, of the colloid rocket can be derived from the usual rocket equations:

$$T = \dot{m}\, v_e \tag{1}$$

$$I_{sp} = v_e / g \tag{2}$$

with $\dot{m}$, the mass flow rate of propellant through the capillary emitter, and v_e, the exhaust velocity, determined from the charge to mass ratio of the formed droplets (q/m), and the applied acceleration potential, ϕ:

$$v_e = \sqrt{2\,(q/m)\,\phi} \tag{3}$$

Experimentally, the charge to mass ratio can be determined from the ratio of the beam emission current, I_b, and the mass flow rate:

$$q/m = \frac{I_b}{\dot{m}} \tag{4}$$

However, an estimate of the most-probable specific charge of the dispersed droplets can be obtained from the Rayleigh criteria:

$$q/m \approx \frac{3\,(\varepsilon_o \gamma)^{1/2}}{\rho r^{3/2}} \tag{5}$$

Here ε_0 is the free space permittivity, γ is the surface tension of the propellant ρ is the density of the propellant, and r is the radius of the droplets. As mentioned above, the droplet charge-to-mass ratio (q/m) can be determined indirectly through the measurement of the beam current and mass flow rate (Eqn. 4). Alternatively it can be estimated through the measurement of the size of the particles and the application of the Rayleigh limiting condition (Eqn. 5). In either case, these estimates can lead to an indirect measurement of the thruster performance. More complicated methods (e.g., mass spectrometry) can be used to determine q/m, although the thrust must still be extracted indirectly. Of course, performance can be determined directly through the use of sensitive thrust stands, although thrust stands that can measure in the μN range are not very common. Below, we describe briefly the use of time-of-flight methods to indirectly determine the thruster performance.

Time-Of-Flight Measurements

Time-of-fight (TOF) diagnostic methods have been routinely used to obtain independent indirect measurements of the properties of colloid sources [2,6]. The TOF characterization method works on the principle that a steady-state ion beam current, when instantaneously interrupted, gives rise to a detected temporal decay in current at a downstream collector that is characterized by the velocity achieved by the ions in-flight at the point of current disruption. The thrust and mass flow rate can be extracted from an analysis of the time-variation in the beam current, $i(t)$, following its disruption at $t = 0$, i.e.:

$$T = \frac{2\phi}{D}\int_0^t i\ \mathrm{d}t \tag{6}$$

$$\dot{m} = \frac{4\phi}{D^2}\int_0^t i\,t\ \mathrm{d}t \tag{7}$$

Here, D is the distance between the emitter and a downstream detector plate, which is assumed to be much larger than the distance between the emitter and the extractor. While TOF methods are based on an ideal description of the beam source (e.g., one-dimensional, monodispersed), they nonetheless provide a means of extracting performance properties based on the measurement of a single system parameter.

Below, we compare the performance measurements taken on a prototype single-emitter CMT propulsion package using the following two methods: (i) from the directly measured "steady-state" beam current and mass flow rate, and (ii) from preliminary TOF diagnostics. Before that, however, we provide the reader with a brief introduction to the nanosatellite on which this CMT package is to fly.

On-Orbit Experiments

The EMERALD nanosatellite project [10] is a two-spacecraft mission, joint between Stanford University and Santa Clara University, and funded through the Air Force Research Laboratory (AFRL) University Nanosatellite Program. Each of the two 20 kg spacecraft is hexagonal in shape measuring 19" in diameter and 12" high. The spacecraft is scheduled for launch in 2003 on board the Space Shuttle. The CMT will be integrated into only one of the EMERALD spacecraft and is expected to provide up to 5 m/s ΔV capability with 10 g of 2.0 M sodium-iodide seeded glycerol propellant, while consuming 6 Watts of maximum total system power. An artist's depiction of the spacecraft pair is shown in **Figure 2**.

To minimize experimental variables, the on-orbit firing of the CMT will involve simple operational

testing monitored by proven methods. The thrust axis of the CMT will be offset from the center-of-gravity of the spacecraft to induce a spin on the satellite during thruster firing. An on-board attitude determination and control system will measure the spin by using light-sensors (earth horizon sensors) and by an analysis of the periodic variation in the solar panel output power.

The research activities at Stanford University are focused primarily on the redevelopment, characterization, and miniaturization of the colloid thruster technology for flight demonstration. The culmination of the research effort is to flight qualify and test a CMT prototype for on-orbit propulsion. The prototype and flight-unit makes use of commercial-off-the-shelf miniature and micro technology (e.g., DC-DC converters, syringe pumps, etc.), and, in some cases, redesigning these technologies for space applications. Such an approach not only brings economic benefit to the project, but also allows for the rapid integration and flight qualification of the experimental package.

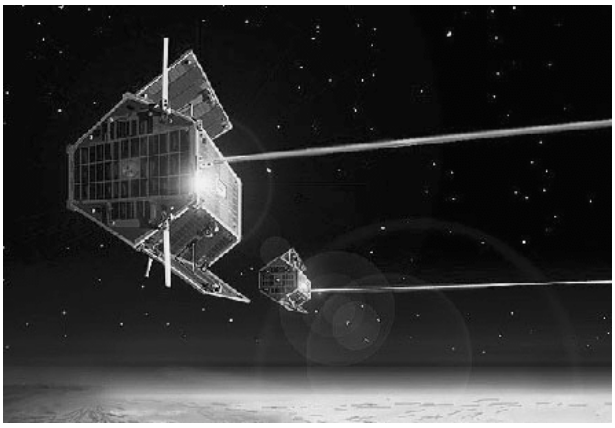

Figure 2. The EMERALD nanosatellite concept.

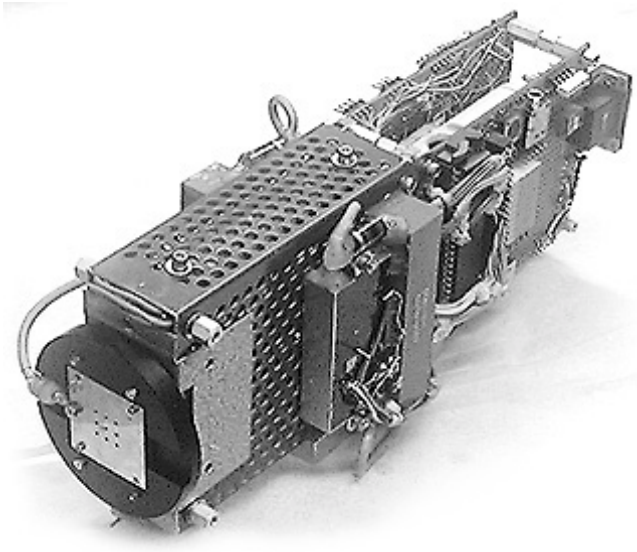

Figure 3. Photograph of the CMT prototype

Experiments

CMT System Description

The CMT system contains a Thruster Control Unit (TCU), Propellant Storage and Delivery Unit (PSDU), and a Thruster Core (TCORE). The prototype CMT is shown in **Figure 3**. The block diagram of the CMT system is shown in **Figure 4**.

The main component of the TCU is a Microchip PIC16F877 microcontroller, which serves as the nerve center of the CMT flight package. The TCU accepts commands via I2C and RS232 serial communications, decodes the commands, and then issues the appropriate analog and digital signals to control the rest of the CMT hardware. The TCU also collects telemetry and data from various sensors (e.g., current, voltage, thermocouple) and transmits the data back to the spacecraft computer. The TCU contains custom software that allows for flexible operation, such as for rapidly switching and reversing the polarity applied to the emitter, or for control of the propellant flow rate.

The PSDU is based on a re-designed miniature portable medical insulin pump, which uses a syringe-plunger mechanism driven by a DC-motor via a high ratio gearbox. The PSDU operation and the flow rate are controlled by the TCU. Redundant latch valves (not yet fully integrated into the prototype package) prohibit premature propellant flow to the TCORE, and are opened once the spacecraft is in orbit.

Three different TCORE assemblies have been studied in our laboratory, although we shall report only on the performance of the single-emitter source in this paper. The single-emitter core assembly has a 150 μm OD / 75 μm ID stainless-steel needle emitter. A multi-emitter array consisting of one hundred of the same needles, as well as a novel, linear-slit core provided by Phrasor Scientific, Inc. of Duarte, CA, are also undergoing tests in our laboratory. The 10 x 10 array is expected to provide 100 times the total thrust obtained

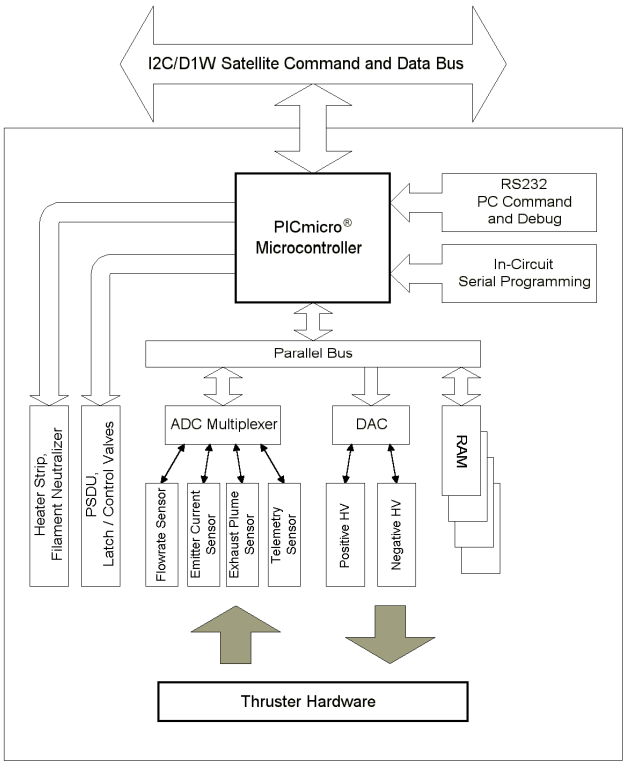

Figure 4. CMT operational block diagram.

from the same single-emitter needle, although preliminary tests indicate that this simple scaling is difficult to achieve in practice, because of both non-uniform propellant delivery, and because of the difficult in the alignment of the needle-guard and extractor orifice.

Vacuum Facility

The experiments were conducted in a 10 cm diameter (vertically oriented), 60 cm long, Pyrex chamber. A base pressure of about 10^{-5} torr is sustained during firing with an Alcatel CFF450 turbopump a backed by Varian mechanical pump. A thermocouple vacuum gauge and an ionization vacuum gauge monitor the coarse and high-vacuum chamber pressures, respectively. **Figure 5** shows a photograph of the CMT vacuum test facility.

In all tests reported on here, the CMT was mounted facing (firing) upward in the chamber. The propellant was a solution consisting of 2M sodium-iodide/ glycerol ($NaI/C_3H_5(OH)_3$), with a measured electrical conductivity of $3.5x10^{-4}$ mho, and a presumed surface tension of $63x10^{-3}$ N/m. A laptop computer handles all commands and data communication to the CMT by way of an RS232 connection via vacuum feedthroughs.

Indirect Thrust Measurements

At present, the facility allows only for an indirect measurement of the thrust and specific impulse, which was implemented for nominal firing conditions using the single-emitter core. The measurement uses the emission current, mass flow rate, and acceleration voltage to calculate the thrust and specific impulse. The second method, based on the TOF, monitors the emission current decay over time immediately following the termination in the acceleration potential.

A collector plate is used to capture the emission current from the CMT. A grounded screen surrounds the collector plate, forming a Faraday cage to help shield the collector from external noise. The collector plate and Faraday cage can be seen in the photograph in **Figure 6**. In this photograph, the thruster (not shown) fires through the rectangular aperture, and the collector is at about a 45^o angle to the incident charged droplet stream. The detector plate is coated with Aquadag® to minimize the perturbation on the beam current due to the secondary electron emission from the collector.

For monitoring the steady-state beam current, the collector plate is connected to a Keithley 487 picoammeter. A Tektronix TDS3014 oscilloscope records the resulting signal output from the picoammeter. In the time-of-flight measurement, a Keithley 417 high-speed current amplifier connected to the collector plate monitors the beam emission current decay. The TDS3014 oscilloscope digitizes and records the resulting time-varying output signal from the current amplifier for data post-processing. The abrupt interruption of the acceleration potential is accomplished by connecting the CMT source plate to ground by way of a high-voltage, low-inductance relay.

An industrial Panasonic CCD camera instrumented with a 50-mm lens was used to image the emission process at the tip of the nozzles with approximately 300x magnification. The image is displayed on a monitor and recorded on a PC for qualitative examination and archiving.

Where possible, the mass flow rate is determined by three independent methods. The first method determines the time-averaged mass flow rate by dividing the mass of the propellant deposited onto the collector by the total thruster operation time. This method requires operation over extended duration, to achieve a measurable amount of change in the collector weight. The second method obtains the mass flow rate by measuring the displacement over time of the meniscus in the propellant line. The third method extracts the mass flow rate directly from the PSDU calibration of the mechanical drive.

Results

The thruster is started from a "cold start" by first slewing the syringe pump, charging the propellant line with fluid to the entrance to the plenum of the emitter core. The PSDU is then instructed to step the motor on the syringe pump to deliver the desired mass flow rate. During this time, the high voltage is applied to the emitter needle. It takes time (~ 10-15 minutes) for the detector plate to first sense the onset of thruster firing. The emission current is first detected as series of repetitive pulses, presumably resulting from a dynamical instability due to propellant starvation at the needle tip. Eventually, the pulses merge into a steady emission current, the level of which depends on the prescribed mass flow rate, and the applied voltage. A typical current trace obtained during a cold start is shown in **Figure 7**. It is noteworthy (and discussed in more detail later in the paper) that upon close inspection, the "pulses" obtained in the early period of the emission process has curious structure which we attribute to the break-up and formation of particles of varying charge-to-mass ratios. Also, the "steady-state" emission seen at long times, is not at all steady, but exhibits fluctuating behavior of low amplitude, superimposed on the DC signal.

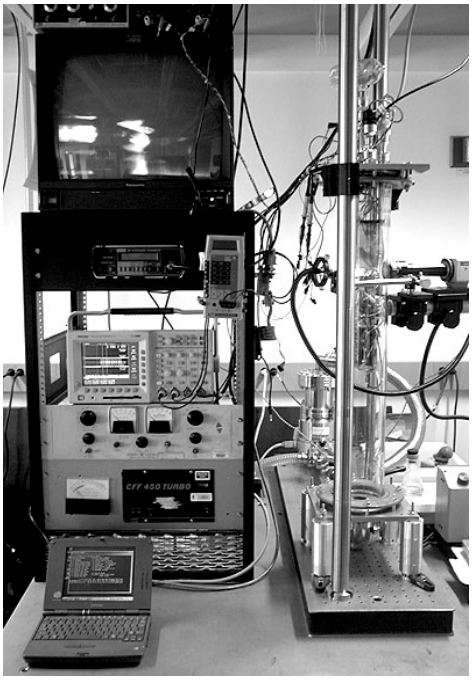

Figure 5. Photograph of the CMT test facility.

Figure 6. Close-up photograph of the detector plate housed within a Faraday cage.

I-V Curve

The measurement of steady-state beam emission current as a function of acceleration potential is presented in **Figure 8**. In general, the thruster beam current is found to increase exponentially with the voltage applied between the source needle and the extractor (acceleration voltage). While the steady-state beam current ranged from 0.1 to 10 μA, bursts with up to 15 μA of current were detected at acceleration potentials of around 5.5-6.0 kV. Note the exponential dependencies of the beam emission current to the acceleration potential. This indicates that the emission process in this source does not obey the theory suggested by Fernandez de la Mora and Loscertales [9], which applies in the limit of large electrical conductivity. That theory also suggests a current that scales as $\sim \dot{m}^{1/2}$, contrary to what we find in our studies. Indeed, as can be seen from Figure 8, the current appears to scale inversely with mass flow rate, with, all else being equal, a higher emission current seen at lower mass flow rate. We do not yet have a

satisfactory explanation for this counterintuitive emission behavior.

At the lower mass flow rate investigated (10^{-9} kg/s), there is an apparent discontinuity in the I-V curve, suggestive of a transition between emission modes. We speculate that below about 4 kV, the process is characterized largely by the emission of sub-micron sized charged drops, of modest charge to mass ratios. Beyond this critical potential, the transition might be indicative of the presence of direct ion emission and/or the emission of high charge to mass ratio droplets. No abrupt transition is seen at the higher mass flow rate (10^{-8} kg/s), although we suspect that such a transition might appear if we were able to operate at higher values of the acceleration voltage.

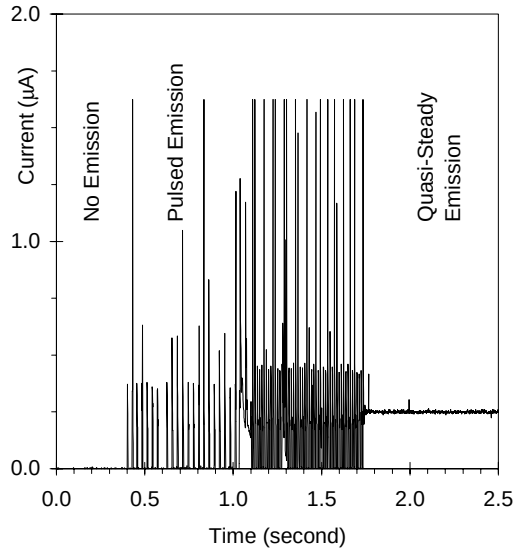

Figure 7. Emission current evolution following cold start.

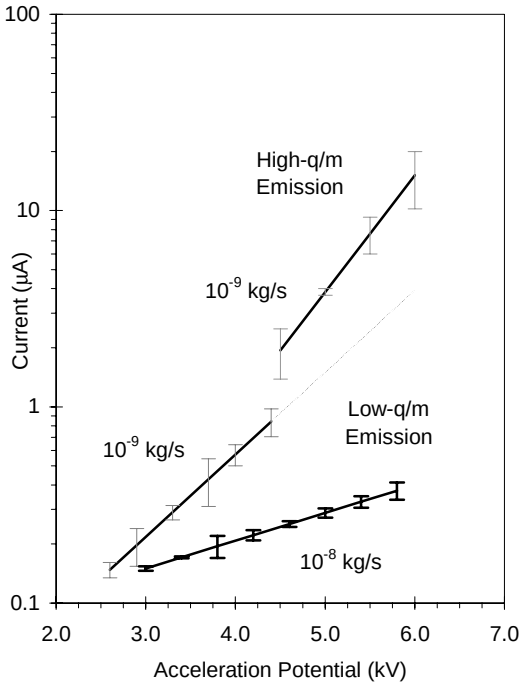

Figure 8. Single-needle beam emission current as a function of acceleration potential.

Performance

The thrust and specific impulse determined by either the "steady state" or TOF methods are given in **Figure 9** and **Figure 10**, respectively. Where TOF data was obtained (see **Figure 9**, for example) thrust calculated using the two different methods agree to within experimental uncertainty. The exponential dependencies of both thrust and specific impulse on the acceleration voltage is also evident here, suggesting the that a simple scaling law might describe the variation in the thrust with applied voltage.

Performance at Lower Mass Flow

With the lower mass flowrate of 10^{-9} kg/sec, as expected, we see an increase in thrust with increased acceleration potential, varying from about 1μN at a potential of 2.6 kV, to 4 μN at a potential of 4.4 kV. A similar trend is seen in the specific impulse, ranging from approximately 60 sec at 2.6 kV, to 200 sec at 4.4 kV. While these values are relatively low for electric rocket technologies, we believe that improved control of propellant flow and field conditions at the nozzle tip for potentials beyond 5 kV can lead to a specific impulse in excess of 400 sec, which is certainly acceptable for a first prototype of this type of rocket. By applying up to 8 kV with reliable propellant control, the current trend suggests that a specific impulse of 1000 sec should be easily attainable. The intermittent 15 μA current bursts which persisted beyond 4.4 kV in acceleration potential resulted in estimated bursts in thrust of approximately 35 μN, and in a specific impulse of about 600 sec, at 6 kV. At present, the origin and cause for these bursts is not well understood.

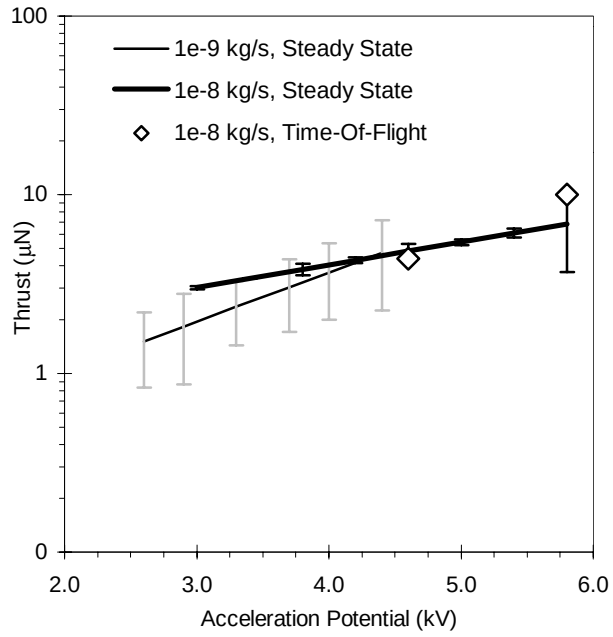

Figure 9. Single-needle core thrust as a function of acceleration potential.

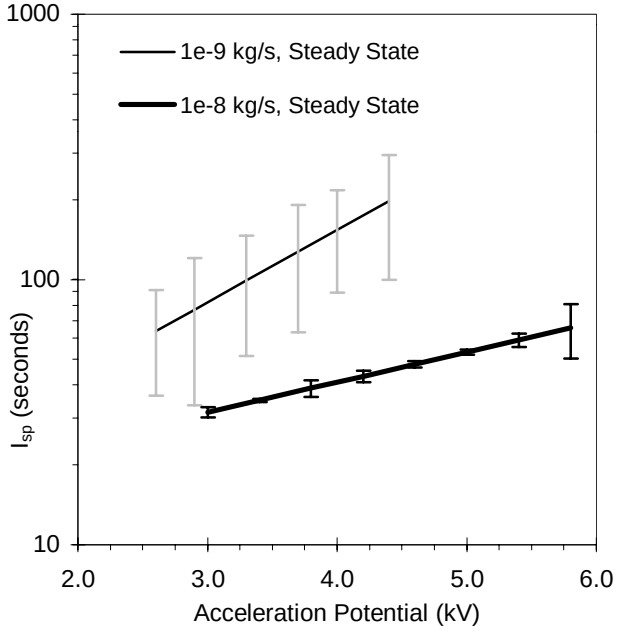

Figure 10. Single-needle core specific impulse as a function of acceleration potential.

Performance at Higher Mass Flow

With the higher mass flowrate setting of 10^{-8} kg/sec, again, as expected we see an exponential increase in thrust with increase in the acceleration potential. The measured thrust using the TOF method is in good agreement with that of the steady-state measurement. Thrust levels vary from about 3 μN at a potential of 3.0 kV, to 8 μN at a potential of 5.8 kV. The specific impulse is also found to vary from approximately 30 seconds at 3.0 kV, to 80 seconds at 5.8 kV. It is noteworthy that the CMT has successfully demonstrated variable thrust and specific impulse operation, controlled largely by independent setting/control of the applied potential and mass flow rate.

While a direct comparison between the low and high mass flow rate is desirable, we note that during the preparations for the experiments with the higher mass flowrate, the distance between the needle emitter and the extractor seemed to be approximately 20% larger than that used in the experiments with the lower mass flowrate. Flooding of the extractor and core would occur (as expected) between experiments when the high voltage is removed, requiring a disassembly of the core, removal of remaining propellant, and a reassembly in preparation of the next experiment. The 20% variation in the emitter-extractor separation is indicative of the reproducibility in the assembly process. Although the acceleration voltage is the same, the 20% increased distance will result in a reduction in field strength, which may contribute to a further reduction (over that caused by the lower mass flow rate itself) in the extracted current.

Particle Break Up

As mentioned earlier, during the initial start of the emission process, prior to achieving a "steady-state" current (most likely due to not yet having established the steady state mass flow), pulsing was observed and attributed to propellant starvation at the needle. The pulsed emission process, although perhaps desirable from a performance standpoint, may provide some insight as to unsteady processes that may occur at the liquid meniscus, and quite possibly, to the break-up of particles during the destabilization of the meniscus, or in flight.

In this pulsed mode, after the initial droplet is extracted from the miniscus, particle break-up can reduce the particle size until the the surface tension of the propellant droplet equals the opposing force between the charged ions on the surface of the particles (the Rayleigh critical charge limit). This

break-up can occur either at the liquid meniscus, in the high electric field region between the emitter and extractor, or in the drift region after the particle passes through the extractor orifice. If the current emission process at the meniscus is rather abrupt and produces a single drop of well defined q/m, any break-up that occurs during the field-free drift should produce a current waveform that is free of high frequency features. However, if break-up occurs between the emitter and extractor, then there will be droplet separation, and possibly droplet interactions that can greatly complicate the detected current waveform.

An expanded view of a single current pulse collected during the initial emission phase is shown in **Figure 11**. Three distinct features are apparent, attributable perhaps to the arrival of three distinct classes of droplets at the downstream collector plate. A sharp peak is first registered, suggesting the early arrival of a class of droplets of well defined and relatively high charge-to-mass ratio. This is followed by a relatively slower cloud of droplets of lower charge to mass ratio. The range over which these droplets arrive at the detector in time (~6 msec), suggests one of three possible scenarios or combinations of: (i) the droplets are of varying charge and of similar size, (ii) the droplets are of the same charge, but varying size, or (iii) the droplets are of the same charge to mass ratio, but experience inter-particle interactions [7,8]. Finally, the peak seen at the trailing edge of the pulse is indicative of the arrival of a small number of slow-moving droplets of well defined but low charge to mass ratios. While a partial explanation for this structure can be speculated on the basis of in-flight particle break-up, at this point, without knowledge that allows us to discern wether the initial microjet emission from the meniscus is free of dynamical features, it is difficult to reach a conclusive interpretation of this pulse shape. Future experiments are planned to monitor the transient current through the circuit just upstream of the emitter. A comparison of this current pulse to that detected can provide some qualitative information as to whether the particles are dispersing at the meniscus, or in flight.

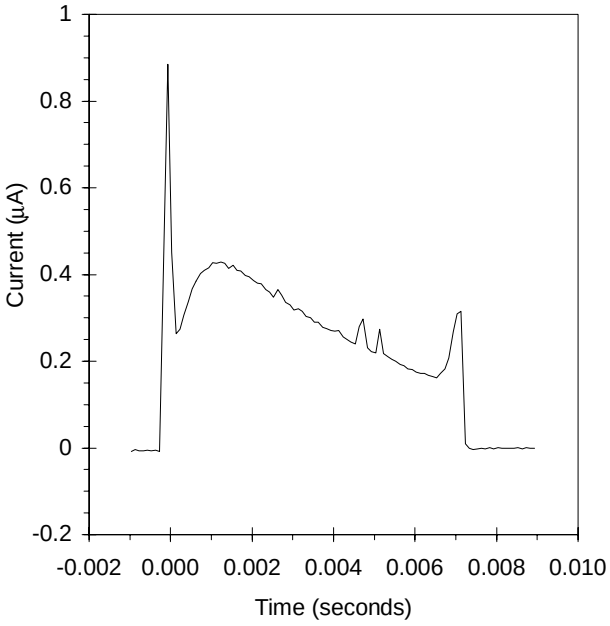

Figure 11. Individual Pulse during Pulsed Emission, indicating the possible presence of three classes of droplets.

Efficiency

While the efficiency of the electrohydrodynamic process itself is expected to be high, also of interest is the *overall system efficiency*, η_{SYSTEM}, which is defined as the ratio of the thruster beam power, $P_{emission}$, to the total system dissipated power, P_{system}, i.e.,

$$\eta_{SYSTEM} = \frac{P_{emission}}{P_{system}} \tag{8}$$

Here, P_{system} includes the power consumption of the microcontroller, its supporting curcuitry, the PSDU, as well as the power losses through the high-voltage power supplies. The system efficiency is affected by numerous factors, but is determined primarily by the efficiency of the high-voltage power supplies and the design of the thruster core.

The efficiency of the high-voltage power supply is dictated by the state of the art of commercial miniature high-voltage power supply, and is therefore considered to be a non-changing variable.

$$\eta_{TCORE} = \frac{P_{emission}}{P_{emission} + P_{loss}} \tag{9}$$

where

$$P_{emission} = \phi \cdot I_b \tag{10}$$

is the emission power as detected by the beam current at the collector, and and where

$$P_{loss} = \phi \cdot I_{loss} \quad (11)$$

with the current loss I_{loss} is defined as:

$$I_{loss} = I_{core} - I_b \quad (12)$$

i.e., the difference between the total current delivered to the thruster core, and that which is actually translated into charged particle beam current, I_b.

Experimental results for η_{TCORE} is shown **Figure 12**. The core efficiency for a single-needle emitter is seen to vary between 20% at 2.6 kV to 40% at 4.4 kV, for the case with 10^{-9} kg/sec mass flowrate. Efficiencies are found to be lower for the higher mass flowrate due to the lower emission currents.

Two primary loss mechanisms are current leakage across the dielectric insulator separating the needle source and the extractor, and emission striking the extractor. Current leakage loss is a function of material used and the design of the insulator, which may be constrained by other performance and system requirements. With proper insulator material selection, the current leakage losses can be made constant throughout the life of the thruster. The extractor strike loss is a function of TCORE design, namely the needle source-extractor arrangement. In addition to reduction in system efficiency, excessive extractor strikes will eventually lead to propellant accumulation and result in electrical shorting between the needle source and the extractor, which potentially may damage the electrodes.

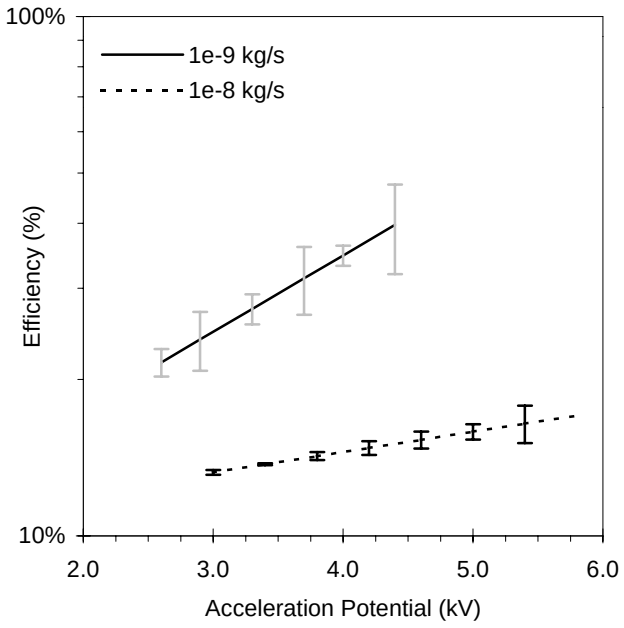

Figure 12. Single-needle thruster core power efficiency, as defined by Eqn. (8).

The experiments reported on above involved the use of a single-nozzle thruster core with a guide electrode, shown in **Figure 13**. This guide electrode serves to better shape the electric field between the emitter needle and the extractor. The addition of this guide electrode led to a significant improvement in performance, in part by reducing the tendency for the emitted electrosray to strike the extractor plate, as shown in **Figure 14**. The guide electrode is maintained at the same potential as the source needle, and in our core design, can be adjusted in position so as to achieve an optimum field distribution.

It is noteworthy that with a thruster core design that employs multiple emitter or emission sites, $P_{emission}$ will be multiplied by the number of emitters or emission sites, while $P_{leakage}$ is expected to remain constant. For a 100 emitter needle array, extrapolating the results for the single-needle core efficiency, the

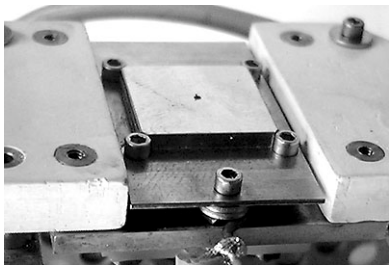

Figure 13. Guide-electrode over the source plate on the single-nozzle thruster core.

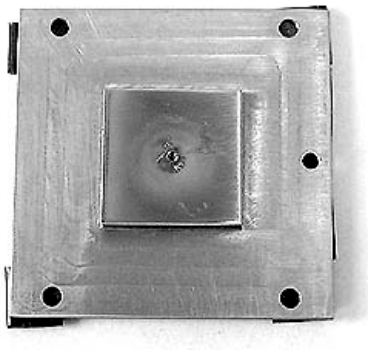

Figure 14. Propellant deposit on extractor plate, operated for extended duration without a guide electrode.

efficiency is expected to be in excess of 90%. The core power efficiency will increase as the number of emitters or emission sites is increased, and if the leakage current across the insulator does not change.

Summary and Discussion

The colloid micro-thruster prototype has operated for more than 100 hours in 10^{-5} Torr vacuum with repeated cold and warm starts. Nominal thrust levels of 0.5-4.0 μN per needle with up to 200 seconds of specific impulse have been recorded and regularly reproduced. Variable thrust and specific impulse was also demonstrated by means of controlling the field strength and the mass flow rate. However higher thrust levels and specific impulse should be attainable at operating voltages higher than our prototype presently provides. Thrust levels up to 35 μN per emitter at higher than 600 seconds specific impulse, corresponding to operation at higher acceleration potential, has been recorded, resulting from intermittent bursts of emission at potentials in excess of 4.4 kV. These conditions are thought to produce emission with higher ionization fraction, with high field strength and reduced mass flowrate as the contributing factor.

Thruster core power efficiency of the single-needle thruster reported on here reaches up to 40%, and is expected to be as high as 90% for the 100-emitter array thruster. The importance of a good thruster core design and its effect on the overall system efficiency and reliability cannot be overemphasized.

Development Challenges

The development effort of the colloid micro-thruster prototype faces a number of unique challenges. The goal to build a flight-qualified thruster, as opposed to a laboratory unit, favors the design to take an integrated system approach, with the resulting design directly applicable to commercial CMT.

The integrated system approach in the design of the CMT also resulted in a much simpler design. This plays a significant role in the qualification of the CMT for flight on board the Space Shuttle. The CMT design has passed the first of three safety reviews by the Space Shuttle Payload Safety Review Panel, and is moving forward toward full flight certification.

One of most difficult challenges is to achieve reliable, extended operation with combined cold and warm starts. The reliable extended operation that has been achieved for the single-needle TCORE, is difficult to achieve with the multiple-needle array. Even though the TCORE array has been operated at a higher emission current and hence thrust (unpublished results), in keeping with the expected scaling, it suffers from serious reliability issues. With the array the alignment between the emitter and the extractor openings is critical in ensuring operation without failure. This is dictated by manufacturing methods and precision in assembly. We have found that even slight misalignment of the extractor/guide electrode/emitter array is enough to affect the field lines so as to cause the particle trajectories to deviate and strike the extractor. Extractor strikes reduces the overall system efficiency, but as important, extended extractor strikes will lead to propellant accumulation eventually results in the shorting of the acceleration potential and system failure.

Acknowledgement

The Colloid Micro-Thruster research project is sponsored by the Air Force as a subcontract on a Phase II STTR project through Phrasor Scientific, Inc. The authors also wish to thank the University Nanosatellite Program and the Nanosatellite support team from AFRL, NASA GSFC and NASA JSC, for their guidance and suggestions. The authors also wish to thank Disetronic Medical Systems, Microchip Technology, Inc. and the Stanford Space Systems Development Laboratory, for their support of this project through donated equipment, or access to facilities and equipment.

References

[1] Mueller, J., AIAA 97-3058, 33rd Joint Propulsion Conference, Seattle, WA, July 1997.

[2] Perel, J., T. Bates, J. Mahoney, R.D. Moore, and A.Y. Yahiku, "Research on a Charged Particle Bipolar Thrustor", AIAA 67-38752.

[3] Mahoney, J., H.L. Daley, and J. Perel, "Performance of Colloid Annular Emitters", AIAA 73-1076

[4] Huberman, M.N, and S.G.Rosen, "Advanced High-Thrust Colloid Sources", Journal of Spacecraft, Vol. 11, No. 7, 1974.

[5] Zafran, S., J.C. Beynon, and P.W. Kidd, "Prototype One-Millipound Colloid Thruster System", AIAA 75-392.

[6] Bailey, Adrian G., "Investigation of a Single Spraying Site of a Colloid Thruster", Journal of Applied Physics, Vol. 6, 1973.

[7] Hendricks, Charles D., and R.J. Pfeifer, "Parametric Studies of Electrohydrodynamic Spraying", AIAA 66-21458.

[8] Bailey, Adrian G., "Electrostatic Spraying of Liquids", Research Studies Press, Ltd., 1988.

[9] De La Mora, J. Fernandez, and I.G. Loscertales, "The Current Emitted by Highly Conducting Taylor Cones", Journal of Fluid Mechanics, Vol. 260, 1994.

[10] Kitts, Christopher A., Robert J. Twiggs, Jonathan How, Freddy Pranajaya, and Bryan Palmintier, "Emerald: A Low Cost Formation Flying Technology Validation Mission", In Proceedings of the 1999 IEEE Aerospace Conference, Snowmass, CO, March 6-13, 1999.